Metabolic-Switch Macrophage Cyborgs Reverse Atherosclerosis by Photoacoustic-Directed On-Demand Phenotype Delivery

Wei Zeng[1], Weimin Fang[1,2], Yuhang Mao[3], Yalan Huang[1,2], Yan Lin[4], Leilei Wu[5], Anqi Chen[6], Zhengan Huang[6], Yuanyuan Sheng[1], Xiaoxuan Lin[1], Jiayu Ye[1], Yanbin Guo[1], Guanxi Wen[1], Jian Zeng[5], Jinfeng Xu[1*], Liqiang Zhou[7,8*], and Yingying Liu[1*]

[1]Department of Ultrasonography, Shenzhen People's Hospital, Second Clinical Medical College of Jinan University, Shenzhen, 518020, China.

[2]Post-doctoral Scientific Research Station of Basic Medicine, Jinan University, Guangzhou 510632, China.

[3]School of Medicine, Ankang University, Ankang, 725000, China

[4]Department of Plastic Surgery, Renmin Hospital of Wuhan University, Wuhan 430060 China.

[5]Department of Thoracic Surgery, Zhejiang Cancer Hospital, Hangzhou Institute of Medicine (HIM), Chinese Academy of Sciences, Hangzhou, 310004, P. R. China.

[6]Guangdong Cardiovascular Institute, Guangdong Provincial People's Hospital (Guangdong Academy of Medical Sciences), Southern Medical University, Guangzhou, 519041, China.

[7]Faculty of Health Sciences, University of Macau, Macau, SAR 999078, PR China

[8]MoE Frontiers Science Center for Precision Oncology, University of Macau, Macau, SAR 999078, PR China

METHODS

1. Flow Cytometric (FC) analysis

Cells were harvested, washed twice with PBS, and resuspended in staining buffer. For surface marker detection, cells were incubated with fluorophore-conjugated antibodies against macrophage and T cells marker at 4°C for 30 min in the dark. When assessing intracellular markers, cells were fixed and permeabilized using a commercial fixation/permeabilization kit according to the manufacturer's instructions before antibody staining. For viability analysis, cells were stained with a live/dead dye prior to antibody incubation. MFO-treated cells were used as the control group. After washing, cells were analyzed using a flow cytometer (BD FACSCanto II, USA), and data were processed with FlowJo software (Version 10.9).

2. Quantitative Real-time PCR (qPCR)

Total RNA was isolated from cells using TRIzol® reagent (Invitrogen, USA) according to the manufacturer's instructions. First-strand cDNA was synthesized with PrimeScript™ RT Master Mix (Takara, China). RT-qPCR was performed on a StepOnePlus Real-Time PCR System (Thermo Fisher Scientific, USA) using TB Green® Premix Ex Taq™ II (Takara, China) with the following cycling conditions: 95°C for 30 s, then 40 cycles of 95°C for 5 s and 60°C for 30 s. β-actin or GAPDH served as the internal reference, and relative expression levels were calculated using the $2^{-\Delta\Delta Cq}$ method. Primer sequences are listed in Table S1.

3. Western blot (WB)

After the treatments, cells were harvested and lysed in RIPA buffer (Beyotime, China). Protein concentrations were measured using a BCA assay kit (Sparkjade, China). Proteins were then separated by SDS-PAGE and analyzed by western blotting following standard protocols.

4. Immunohistochemistry (IHC)

Frozen arterial sections (8 μm) were fixed with cold PFA, and endogenous peroxidase activity was blocked. After blocking non-specific binding, sections were incubated overnight at 4°C with the appropriate primary antibody, followed by incubation with an enzyme-conjugated secondary antibody. Target proteins were visualized using DAB chromogen and counterstained with hematoxylin. The stained area was quantified independently using threshold-based analysis in Image Pro Plus software (Version 6.0).

RESULTS

Table S1. Primer sequences.

Gene	Forward (5'-3')	Reverse (5'-3')
Arg-1	CATTGGCTTGCGAGACGTAGAC	GCTGAAGGTCTCTTCCATCACC
iNOS	GAGACAGGGAAGTCTGAAGCAC	CCAGCAGTAGTTGCTCCTCTTC
Ym-1	CAGCTGGACATGGACACATT	TTGCTCAGGTTGGTGTTTGT
TNF-α	GGTCCCCAAAGGGATGAGAAG	CACTTGGTGGTTTGTGAGTGTG
ABCA1	GGAGCCTTTGTGGAACTCTTCC	CGCTCTCTTCAGCCACTTTGAG
ABCG1	GACACCGATGTGAACCCGTTTC	GCATGATGCTGAGGAAGGTCCT
CD36	GGACATTGAGATTCTTTTCCTCTG	GCAAAGGCATTGGCTGGAAGAAC
ACTB	CATTGCTGACAGGATGCAGAAGG	TGCTGGAAGGTGGACAGTGAGG
GAPDH	CATCACTGCCACCCAGAAGACTG	ATGCCAGTGAGCTTCCCGTTCAG

Table S2. Comparative summary of recent cell-based AuNP/microbubble platforms and the present study.

Ref (DOI)	Carrier type	Imaging modality	Triggering mechanism	Metabolic target	Functional output (reported)
Chen et al., Atherosclerosis (2024) 10.1016/j.atherosclerosis.2023.117423	SR-A-targeted Ce6 nanobubbles	Fluorescence imaging (for targeting)	Sonodynamic therapy (LIPUS)	—	Plaque reduction (39.08% vs control); M1→M2 polarization
Alva et al., Nat Commun (2025) 10.1038/s41467-025-61624-1	Lipid-shelled macrophage-labeled microbubbles	B-Mode and AMPI	Low mechanical index (MI < 0.34) ultrasound pulses	—	Single-cell macrophage imaging; in vivo macrophage tracking
Chen S. et al., Sci Adv (2025) 10.1126/sciadv.adw7191	Macrophages with surface-attached β-elemene-loaded GeS nanosheets	Bioluminescence and fluorescence imaging	Sonodynamic therapy (LIPUS)	Immunometabolism modulation	↑ Tumor suppression (92%); immune remodeling
Chan H.-W. et al., Mater Today Bio (2025) 10.1016/j.mtbio.2025.102029	AuNPs (radiolabeled with ^{131}I)-loaded macrophages	Nope (Pre-labeled with LT-810™ for fluorescence imaging *in vivo*)	X-ray radiotherapy (8 Gy, AuNPs only used for radiosensitizers)	Radiosensitization and immune remodeling	↑ Tumor suppression (92%); ↑ Macrophages (2.3-fold); ↑ NK cells (2.4-fold); ↑ $CD8^+$ T cells (3.8-fold)
Our work (MφMB-Au)	Macrophage + PEI-coated microbubbles carrying AuNPs	Dual-modal real-time tracing (Ultrasound + Photoacoustic)	Ultrasound-triggered AuNP release, then promotes M2 polarization	ABCA1-mediated cholesterol–fatty-acid metabolism	Plaque reduction (54.48% vs control); ↓M1/M2 ratio (83.53%), ↑ Treg (2.7-fold), ↑plaque vulnerability

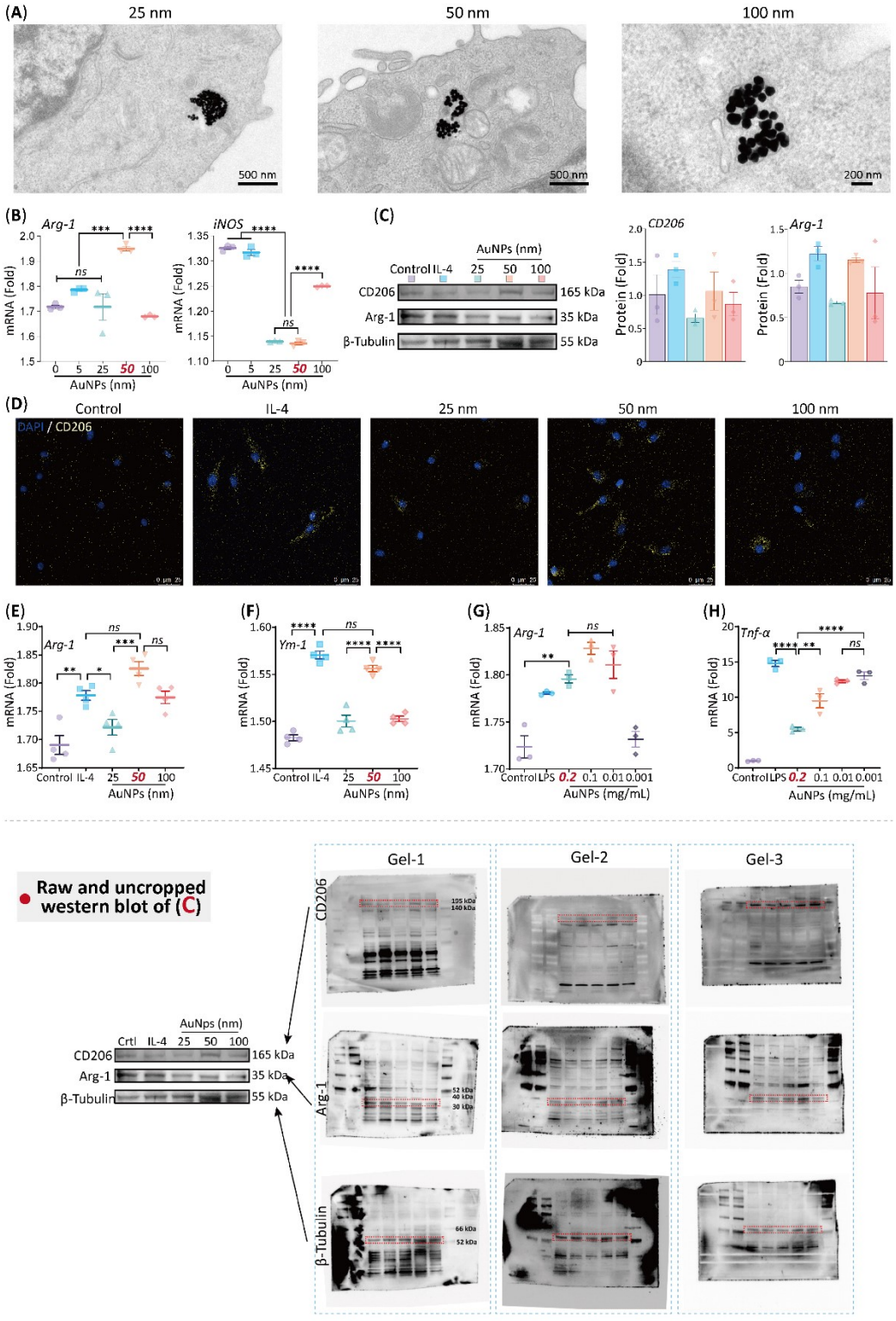

Figure S1. AuNPs size/concentration screening and M2 polarization (**A**) TEM images of macrophage-internalized AuNPs (25, 50, 100 nm). (**B**) mRNA expression of Arg-1 and iNOS after co-incubation with AuNPs of different sizes. (**C**) WB analysis of Arg-1 and CD206 protein levels. (**D**) CD206 fluorescence expression following AuNP treatment. (**E-F**) qPCR analysis of M2-related genes Arg-1 and Ym-1. (**G-H**) qPCR analysis showing increased Arg-1 and reduced TNF-α expression in response to graded concentrations of 50 nm AuNPs.

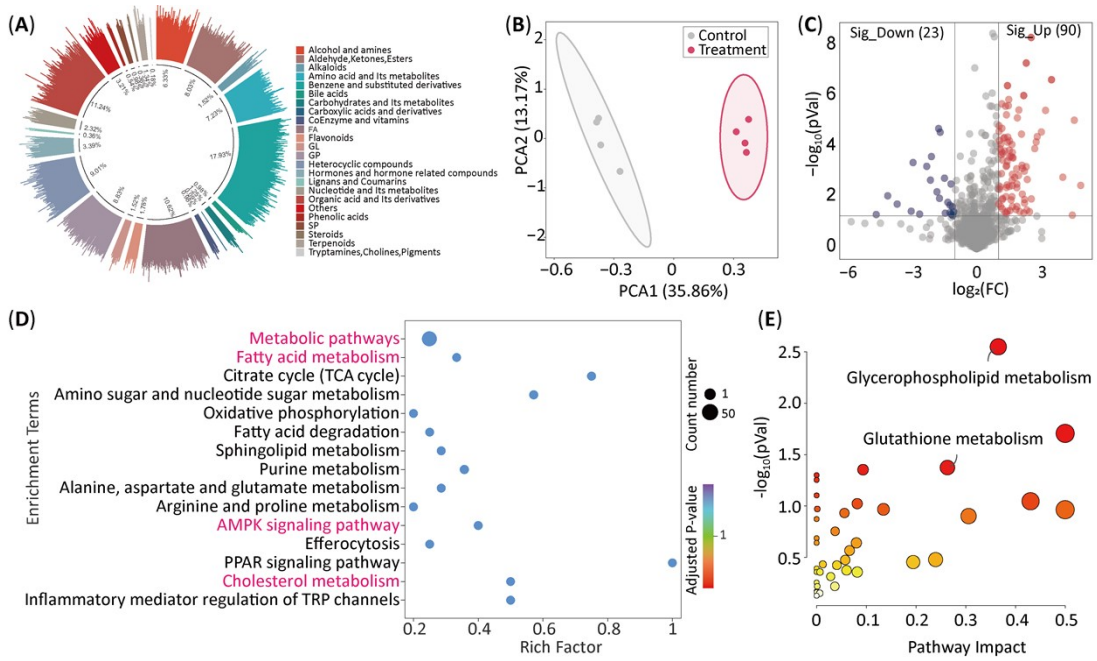

Figure S2. The metabolomic analysis of AuNPs on macrophages. (**A**) Circle diagram for the distribution of metabolites. (**B**) PCA score plot showing differences between the control and the treatment groups. (**C**) Volcano plot demonstrating altered metabolite levels. Fold Change < 0.5 / > 2 and *P*-value < 0.05. (**D**) KEGG pathway enrichment analysis based on the LC-MS metabolomics assay. (**E**) Pathway analysis of significant differential metabolites.

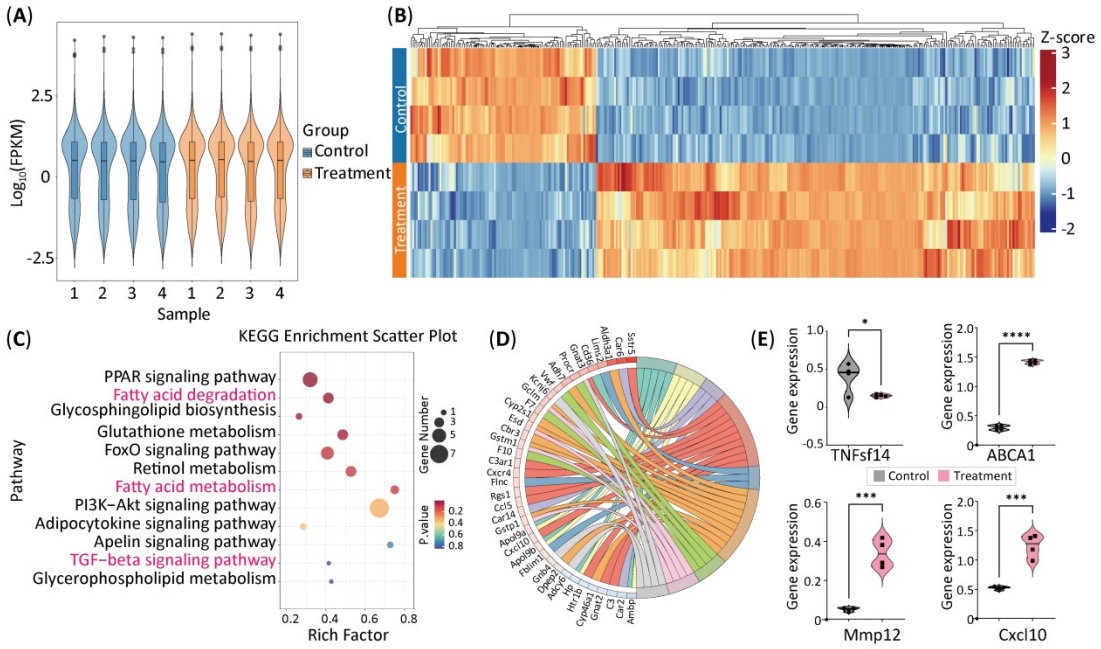

Figure S3. The transcriptomic analysis of AuNPs on macrophages. (**A**) Violin plot illustrating the distribution of control and treatment samples. (**B**) Heatmap for the distribution of genes. (**C**) KEGG pathway enrichment analysis. (**D**) Reactome pathway enrichment chord diagram. (**E**) Bar chart showing the statistics of differentially expressed genes.

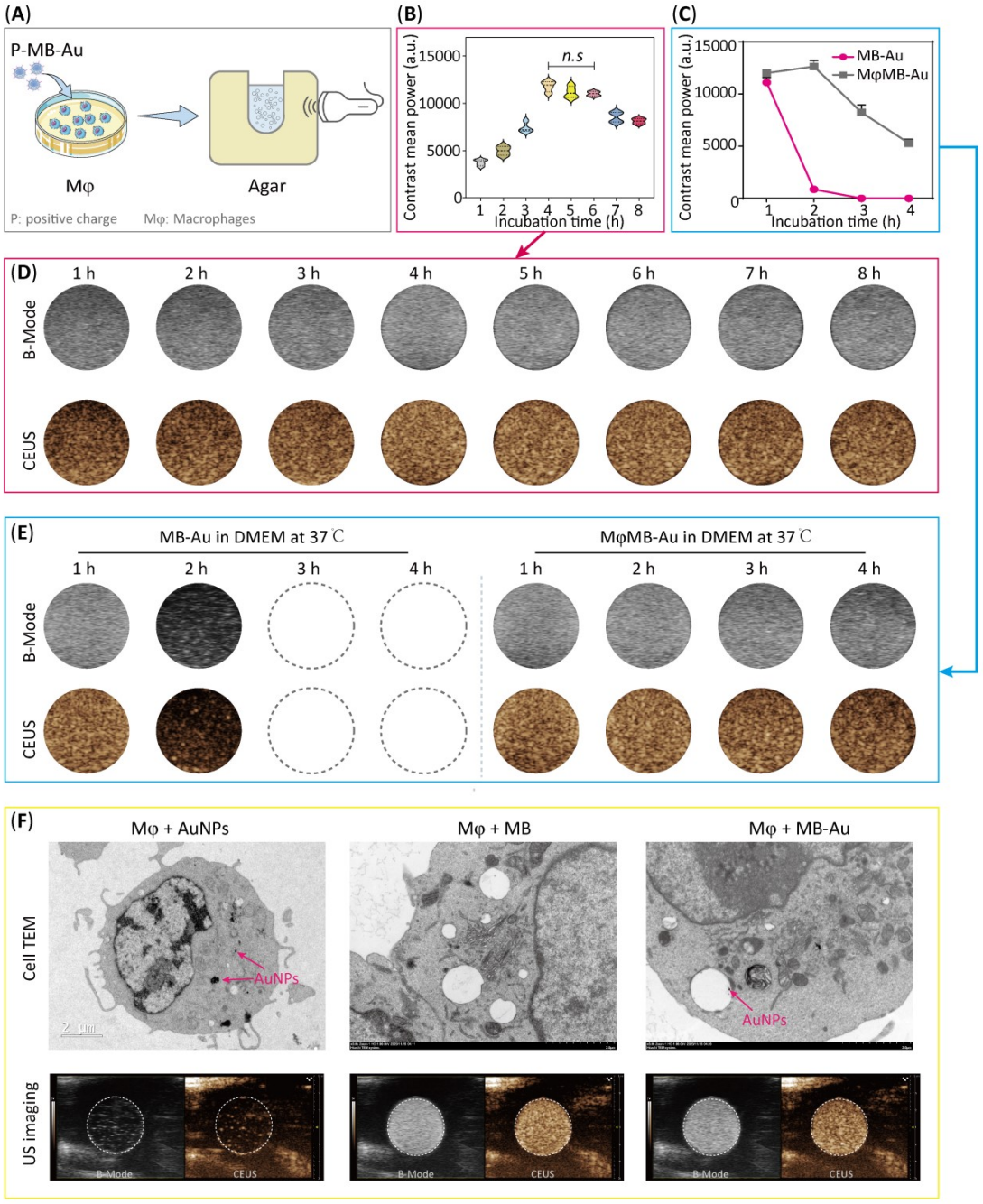

Figure S4. Ultrasonic imaging *in vitro*. (**A**) Schematic illustration of P-MB-Au co-incubation with macrophages and subsequent ultrasound imaging. (**B, D**) Ultrasound imaging of macrophages co-incubated with MB-Au at different time points, along with quantitative statistical analysis. (**C, E**) Time-course ultrasound imaging of MφMB-Au and MB-Au in DMEM at 37°C, along with quantitative statistical analysis. (**F**) TEM images and CEUS imaging of macrophages after co-incubation with AuNPs, MB, or MB-Au.

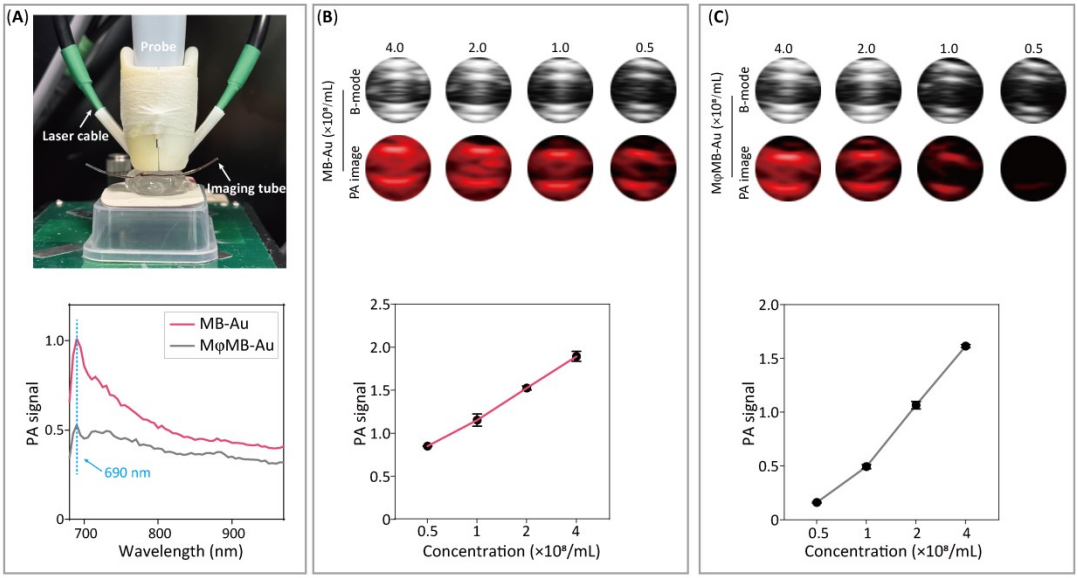

Figure S5. Photoacoustic imaging *in vitro*. (**A**) Schematic illustration of photoacoustic (PA) imaging (top) and characteristic PA signal peaks of MB-Au and MφMB-Au (bottom). (**B-C**) PA images and corresponding quantitative analysis of MB-Au and MφMB-Au at various concentration gradients, respectively.

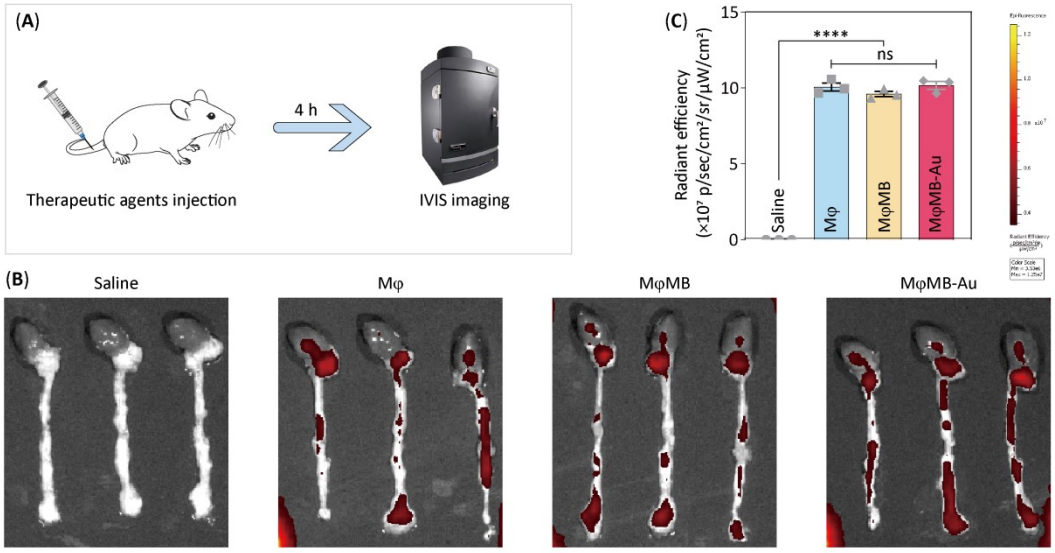

Figure S6. Impact of macrophage engineering on inflammatory targeting capacity. (**A**) Schematic illustration of the experiment. Mφ, MφMB, and MφMB-Au were labeled with DiR. Four hours after labeling, mice were euthanized, and the heart together with the attached aorta was collected for ex vivo small-animal imaging. (**B**) Representative IVIS fluorescence images of each group. (**C**) Quantification of fluorescence signals. *$p < 0.05$, **$p < 0.01$, ***$p < 0.001$, ****$p < 0.0001$.

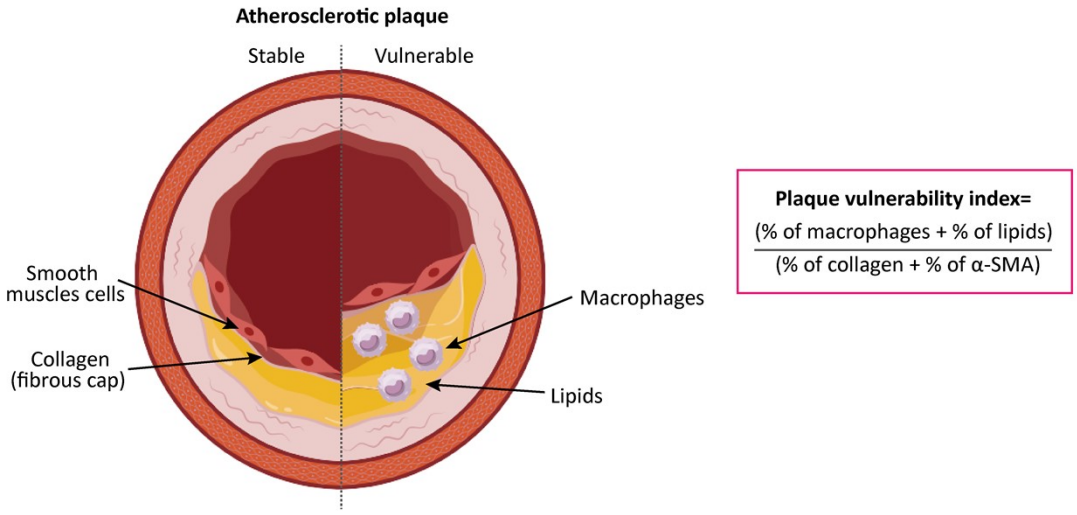

Figure S7. Schematic of stable and vulnerable plaques, and calculation formula for plaque vulnerability index (PVI).

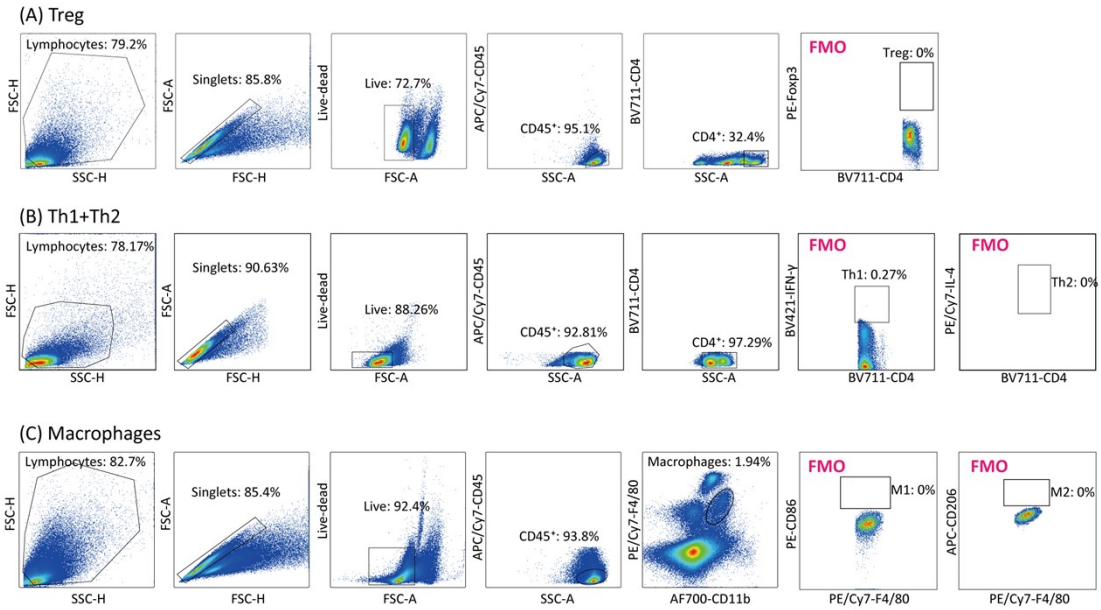

Figure S8. Representative gating strategy used for flow cytometry data acquisition and analysis. Initial gates were applied on forward scatter (FSC) versus side scatter (SSC) plots to exclude debris and select the main cell population. Singlets were then identified by FSC-H versus FSC-A gating to exclude doublets. Subsequently, live cells were gated using viability dye exclusion. Specific cell populations were identified based on the expression of surface markers. Fluorescence Minus One (FMO) control was used to define the boundaries between positive and negative populations, ensuring accurate gating and minimizing false positives due to spectral overlap or background fluorescence. This gating strategy was applied consistently across all experimental groups to ensure reliable and comparable data interpretation.

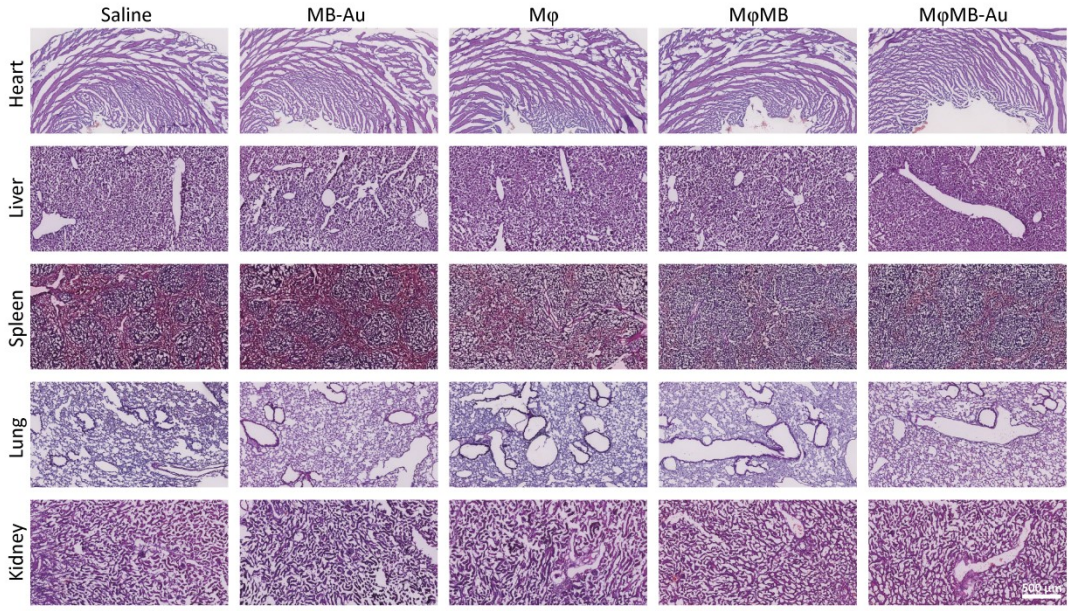

Figure S9. Safety assessment after treatment. HE staining of major organs in each group of mice.